

Magnetic heat transport in $R_2\text{CuO}_4$ ($R = \text{La, Pr, Nd, Sm, Eu, and Gd}$)

K. Berggold, T. Lorenz, J. Baier, M. Kriener, D. Senff, H. Roth, A. Severing, H. Hartmann, and A. Freimuth
II. Physikalisches Institut, Universität zu Köln, Zülpicher Str. 77, 50937 Köln, Germany

S. Barilo

*Institute of Solid State & Semiconductor Physics,
 Belarussian Academy of Sciences, Minsk 220072, Belarus*

F. Nakamura

Department of Quantum Matter, ADSM, Hiroshima University, Higashi-Hiroshima, 739-8526 Japan

(Dated: August 12, 2018)

We have studied the thermal conductivity κ on single crystalline samples of the antiferromagnetic monolayer cuprates $R_2\text{CuO}_4$ with $R = \text{La, Pr, Nd, Sm, Eu, and Gd}$. For a heat current within the CuO_2 planes, i. e. for κ_{ab} we find high-temperature anomalies around 250 K in all samples. In contrast, the thermal conductivity κ_c perpendicular to the CuO_2 planes, which we measured for $R = \text{La, Pr, and Gd}$, shows a conventional temperature dependence as expected for a purely phononic thermal conductivity. This qualitative anisotropy of κ_i and the anomalous temperature dependence of κ_{ab} give evidence for a significant magnetic contribution κ_{mag} to the heat transport within the CuO_2 planes. Our results suggest, that a large magnetic contribution to the heat current is a common feature of single-layer cuprates. We find that κ_{mag} is hardly affected by structural instabilities, whereas already weak charge carrier doping causes a strong suppression of κ_{mag} .

PACS numbers: PACS numbers: 74.72.-h, 66.70.+f

I. INTRODUCTION

Various low-dimensional spin systems show an unusual thermal conductivity κ with a double-peak structure as a function of temperature. There is growing evidence that this anomalous behavior arises from magnetic excitations contributing to the heat transport. The most clear experimental evidence is found in the spin-ladder compounds, where a double-peak structure with a huge high-temperature maximum of κ is present for a heat current parallel to the ladder direction, but absent for a heat current perpendicular to the ladders.^{1,2} For one-dimensional spin-chain systems the experimental results are less clear. For the spin-chain compounds SrCuO_2 and Sr_2CuO_3 Sologubenko *et al.* find a sizeable extra contribution to κ along the chain direction, which is missing in the other directions.³ In the spin-Peierls compound CuGeO_3 κ along the chain direction has two low-temperature maxima and one of them was attributed to a magnetic contribution in Ref. 4. However, this interpretation is questionable, because a similar double peak is also present in κ perpendicular to the chain direction.⁵ For the Haldane-chain ($S = 1$) System AgVP_2S_6 , a magnetic contribution seems to play a role too,⁶ but the absolute values are much smaller than in the $S = 1/2$ systems. The results in 1D systems raise the question whether a sizeable heat current due to magnetic excitations is also present in two-dimensional magnets. This was discussed for the low-temperature thermal conductivity of $\text{K}_2\text{V}_3\text{O}_8$ and Nd_2CuO_4 .^{7,8,9} The latter is one of the insulating parent compounds of high-temperature superconductors containing CuO_2 planes, which represent the perhaps most studied two-dimensional antiferromagnets

so far.¹⁰ Whereas the studies on Nd_2CuO_4 (Refs. 8,9) mainly concern the magnetism of the Nd^{3+} moments, the influence of the Cu^{2+} moments is present at higher temperature. In the layered perovskite La_2CuO_4 , the thermal conductivity κ_{ab} for a heat current along the CuO_2 planes exhibits a pronounced double-peak structure with a low-temperature maximum around 25 K and a second one around 250 K. In contrast, the thermal conductivity κ_c perpendicular to the CuO_2 planes has only one low-temperature peak.^{11,12,13,14} These findings have been interpreted in terms of an additional heat transport parallel to the CuO_2 planes due to magnetic excitations. However, a double-peak structure can also be explained by phonons only. Any additional scattering mechanism which acts in a narrow temperature range suppresses κ in that temperature window and as a result κ may exhibit two peaks. For example, in $\text{SrCu}_2(\text{BO}_3)_2$ a double-peak structure is caused by resonant scattering of acoustic phonons by magnetic excitations.¹⁵ Such a mechanism does not apply for La_2CuO_4 . However, La_2CuO_4 has a structural instability with low-lying optical phonon branches, which could also serve as scatterers for the acoustic phonons. Such an explanation has been proposed by Cohn *et al.* for the heat transport data of $\text{YBaCuO}_{6+\delta}$, which show a similar temperature dependence of κ_{ab} as La_2CuO_4 .¹⁶

Recently, we have measured κ_{ab} of $\text{Sr}_2\text{CuO}_2\text{Cl}_2$ in order to investigate the possibility that resonant phonon scattering due to the structural instability may cause the double-peak structure in κ_{ab} of La_2CuO_4 . $\text{Sr}_2\text{CuO}_2\text{Cl}_2$ and La_2CuO_4 are almost isostructural, but $\text{Sr}_2\text{CuO}_2\text{Cl}_2$ has no structural instability. Nevertheless we also found a second high-temperature maximum in κ_{ab} and took this

as evidence for the second peak of the in-plane heat conductivity being caused by magnetic excitations.¹⁷ Basing on this observation we expect that a pronounced magnetic contribution to the thermal conductivity is a common feature of the layered cuprates. However, the high-temperature peak of κ_{ab} of La_2CuO_4 is significantly larger and its low-temperature peak is much smaller than the corresponding peaks observed in $\text{Sr}_2\text{CuO}_2\text{Cl}_2$. These quantitative differences could arise from the absence or presence of a structural instability and/or weak charge carrier doping in the different samples. In order to investigate whether the high-temperature peak of κ_{ab} is indeed an intrinsic feature of the antiferromagnetic CuO_2 planes and to get more insight about the influence of structural changes, we have studied the thermal conductivity on single crystals of $R_2\text{CuO}_4$ with different rare earths R , which realize different structures. Some of these compounds even show a structural transition as a function of temperature.^{18,19,20,21} Up to now only the in-plane thermal conductivity for $R = \text{Pr}$ and Nd has been studied,^{8,9,22,23} and the studies of κ_{ab} and κ_c of La_2CuO_4 have concentrated on the influence of doping.^{11,12,13,14}

Here, we present measurements of κ_{ab} for $R = \text{Pr}$, Nd , Sm , Eu , and Gd and of κ_c for $R = \text{Pr}$ and Gd . Our study clearly shows that the anomalous double-peak structure of κ_{ab} is present for all $R_2\text{CuO}_4$ and confirms that a large magnetic contribution to the heat transport is an intrinsic property of the CuO_2 planes. In addition, we find that this magnetic contribution is hardly affected by a structural instability while the phononic contribution is strongly suppressed.

II. MAGNETIC AND STRUCTURAL PROPERTIES OF $R_2\text{CuO}_4$

A common feature of La_2CuO_4 and $R_2\text{CuO}_4$, with $R = \text{Pr}$, Nd , Sm , Eu , and Gd is the layered structure with planes consisting of a CuO_2 square lattice. These planes are a good realization of a two-dimensional antiferromagnetic $S = \frac{1}{2}$ Heisenberg square lattice. Bi-magnon Raman scattering²⁴ yields exchange constants J between $\approx 1200 - 1400$ K for $T = 300$ K given in Table I.²⁵ Finite inter-plane couplings J_{\perp} lead to three-dimensional antiferromagnetic ordering with Néel temperatures of $T_N \approx 250 \dots 320$ K (see Table I). In general, the ordering temperature is determined by the ratio of the inter- and the intra-plane coupling. However, crystal quality and the oxygen stoichiometry strongly influence T_N , too. For example, very small amounts of excess oxygen drastically suppress T_N of $\text{La}_2\text{CuO}_{4+\delta}$.²⁶ Apart from the magnetic Cu subsystem, the compounds with magnetic rare earth ions R contain another magnetic subsystem. In all these compounds the behavior of the Cu subsystem is very similar. However, the details of the magnetic structure are determined by the competition between the different couplings (Cu-Cu, R - R , R -Cu).^{27,28}

La_2CuO_4 crystallizes in the so-called T structure (also

called K_2NiO_4 structure). The CuO_4 plaquettes of the planes and the apex oxygen ions form CuO_6 octahedra. At high temperatures La_2CuO_4 is in the high-temperature tetragonal phase (HTT phase). At 530 K a structural phase transition takes place,¹⁹ where the octahedra tilt leads to the low-temperature orthorhombic phase (LTO), which is stable down to lowest temperature. Due to the octahedron tilt the point bisecting the nearest neighbor Cu-Cu distance is no longer a center of inversion symmetry giving rise to a Dzyaloshinski-Moriya (DM) type interaction. $\text{Sr}_2\text{CuO}_2\text{Cl}_2$ is almost isostructural to La_2CuO_4 with the La^{3+} ions being substituted by Sr^{2+} and the apex O^{2-} by Cl^{-} ions. In $\text{Sr}_2\text{CuO}_2\text{Cl}_2$ the HTT phase is stable down to the lowest temperature and due to inversion symmetry no DM exchange and consequently no spin canting occurs. The $R_2\text{CuO}_4$ compounds crystallize in the tetragonal so-called T'-structure. While the T structure may be viewed as a stacking of one CuO_2 layer followed by two LaO (or SrCl) layers, the stacking of the T' structure is one CuO_2 layer followed by a layer of R^{3+} ions, a layer of O^{2-} ions, and finally another layer of R^{3+} ions. Consequently, there are no apex oxygen ions present in the T' structure and the basic building blocks are CuO_4 plaquettes instead of the CuO_6 octahedra of the T structure. For $R = \text{Pr}$, Nd , and Sm the T' structure is stable over the entire temperature range. For Eu_2CuO_4 and Gd_2CuO_4 structural phase transitions are observed with transition temperatures of 170 K and 685 K, respectively.^{20,21} The structural changes can be described by an alternating rotation of the CuO_4 plaquettes around the c axis. The rotation angles amount to 2.3° at 20 K for $R = \text{Eu}$ and to 5.2° at 300 K for $R = \text{Gd}$.^{20,21} The structural transitions transform both the T and the T' structure into orthorhombic structures, but all these crystals are usually strongly twinned with respect to the a and the b axes. As in La_2CuO_4 , the lower symmetry in the distorted T' phases gives rise to a DM interaction and leads to a canting of the magnetic moments.

III. EXPERIMENTAL

The $R_2\text{CuO}_4$ single crystals were grown in Pt crucibles by the top-seeded solution method as described in Ref. 33. The La_2CuO_4 crystal was grown by a traveling-solvent floating zone method. The finite DM interaction for $R = \text{La}$ and Gd causes a weak ferromagnetic moment, which allows an easy determination of the Néel temperature T_N by measurements of the magnetic susceptibility χ . For $R = \text{Gd}$ we find $T_N \simeq 292$ K in agreement with the highest values reported for Gd_2CuO_4 .^{34,35} Our $\text{La}_2\text{CuO}_{4+\delta}$ single crystal has a comparatively low $T_N = 245$ K due to excess oxygen. A comparison of the in-plane resistivity (not shown) with Ref. 36 yields $\delta \approx 0.01$. The determination of T_N from $\chi(T)$ does neither work in the undistorted samples with $R = \text{Pr}$, Nd , and Sm , since there is no weak ferromagnetism nor for

TABLE I: Exchange constants J at 300 K (Ref. 24), Debye temperatures Θ_D , sound velocities v_s , sample sizes, and Néel temperatures T_N of $R_2\text{CuO}_4$ (see text and the respective references). P , D , U , and u are fit parameters for the fits of the phononic contribution of κ . P and D describe the scattering on point defects and planar defects, respectively, whereas U and u model Umklapp scattering (for details see Ref. 17). If available, the values for Θ_D and v_s are taken from literature, otherwise similar values have been used for the fits.

	J (K)	Θ_D (K)	v_s (m/s)	$a \times b \times c$ (mm 3)	T_N (K)	P (10 $^{-43}$ s 3)	D (10 $^{-18}$ s)	U (10 $^{-31}$ s 2 /K)	u
La_2CuO_4 <i>ab</i>	(Ref. 11)	1465	385 (Ref. 29)	5200 (Ref. 30)	316	21	26	22	4.4
La_2CuO_4 <i>ab</i>	(Ref. 12)				323	1.5	11.8	23	5.3
La_2CuO_4 <i>ab</i>	(Ref. 12)				313	23.8	4.6	14.1	7
La_2CuO_4 <i>ab</i>	(Ref. 13)				308	25.8	26.2	15.3	4.4
La_2CuO_4 <i>c</i>	(Ref. 11)				316	15.4	14.6	17.3	6.4
La_2CuO_4 <i>c</i>	(Ref. 12)				325	1.9	15.1	18.8	5.5
$\text{La}_2\text{CuO}_4\delta$				0.6 \times 3 \times 2.5	245				
Pr_2CuO_4 <i>ab</i>		1243	361 (Ref. 31)	6000 (Ref. 32)	1.7 \times 1.6 \times 1.4	250	7.1	1	8.5
Pr_2CuO_4 <i>c</i>						10.3	2.0	13.0	5
Nd_2CuO_4 <i>ab</i>		1248	319 (Ref. 31)	5900 (Ref. 32)	2 \times 1 \times 0.3		5	10.7	11.0
Nd_2CuO_4 <i>ab</i>	(Ref. 8)				275	0.27	11.1	9.6	4
Sm_2CuO_4 <i>ab</i>		1300	353 (Ref. 31)	5900	3.2 \times 3.7 \times 0.4		1.2	16.5	21.2
Eu_2CuO_4 <i>ab</i>		1300			2.6 \times 2 \times 0.3				5.2
Gd_2CuO_4 <i>ab</i>	A	1292	350	5900	2 \times 0.7 \times 1.1	290	11	17.5	2.4
Gd_2CuO_4 <i>c</i>	A						7.6	40.1	3.5
Gd_2CuO_4 <i>ab</i>	B				1.6 \times 0.9 \times 0.4	295	8.3	10.6	3.1
								2.6	5

$R = \text{Eu}$, where the structural transition takes place well below T_N . According to Ref. 8 there is a slope change of χ_{ab} at T_N in Nd_2CuO_4 , but we could not reproduce such a feature in χ_{ab} of our crystal. For Pr_2CuO_4 we determined $T_N \simeq 250$ K at the Laboratoire Leon Brillouin, Saclay by neutron diffraction, which is well below the maximum values up to $T_N \simeq 280$ K reported for this compound.^{37,38,39} Unfortunately, our Nd_2CuO_4 crystal is too small for neutron diffraction and this method cannot be applied for $R = \text{Eu}$ and Sm because of the large neutron absorption cross section of these elements.

All crystals have been oriented using a Laue camera and cut into rectangular pieces. Sample sizes are listed in Table I. The accuracy of the orientation with respect to the crystal axes is about 2°. Since the Sm_2CuO_4 crystal has approximately the shape of a cuboid, it has not been cut. Here, the misalignment amounts to $\simeq 10$ °. The shape of Pr_2CuO_4 and Gd_2CuO_4 allowed measurements of κ_c with a heat current j_H parallel to the *c* axis, i.e. perpendicular to the CuO_2 planes, and of κ_{ab} with j_H within the CuO_2 planes. For $R = \text{Nd}$, Sm , and Eu , we could only measure κ_{ab} , because these crystals were very thin with lengths of less 0.4 mm parallel to the *c* axis. For $R = \text{Pr}$, Nd , and Gd we measured κ_{ab} with j_H parallel to the *a'* axis of the HTT phase, which has an angle of 45° with respect to the orthorhombic *a* and *b* axes. For $R = \text{Eu}$ and Sm j_H had an arbitrary orientation with respect to the *a* and *b* axes.

The thermal conductivity has been measured by a standard steady-state method. One end of the sample has been attached to the sample holder by silver paint and a small resistor has been glued to the opposite end of the sample by an insulating varnish (VGE-7031, LakeShore). The temperature of the sample holder has been stabilized and an electrical current through the resistor has been used to produce a heat current through

the sample. The resulting temperature gradient has been determined by a differential Chromel-Au+0.07%Fe-thermocouple, which has been also glued to the sample. Typical temperature gradients were about 0.5% of the sample temperature. The absolute accuracy of our method is restricted to about 10% because of uncertainties in determining the sample geometry and, in particular, the exact distance between the two ends of the thermocouple. The relative accuracy is about one order of magnitude better. Radiation losses are negligible for our sample geometry.

IV. RESULTS

A. Gd_2CuO_4 and Pr_2CuO_4

Figure 1 shows the thermal conductivity of Gd_2CuO_4 measured on two different samples. One sample allowed to measure κ_{ab} and κ_c , whereas the second crystal was too thin to measure κ_c . In Figure 2 we display κ_{ab} and κ_c of Pr_2CuO_4 . Apart from differences around the low-temperature maximum, which is very sensitive to the sample quality, our data agree well to the previously reported κ_{ab} of Pr_2CuO_4 .²³ For both compounds κ_c follows the typical temperature dependence of the thermal conductivity of acoustic phonons. As shown by the solid lines, κ_c can be reasonably well described within a Debye model. We use the same model and nomenclature as in our previous publication (see Eqs. (1) and (2) of Ref. 17) and the corresponding fit parameters are given in Table I. In both crystals κ_{ab} exceeds κ_c over the entire temperature range. The low-temperature maxima for Gd_2CuO_4 are slightly shifted in temperature. The most striking anisotropy is, however, the additional, broad maximum of κ_{ab} around 250 K. Although the low-

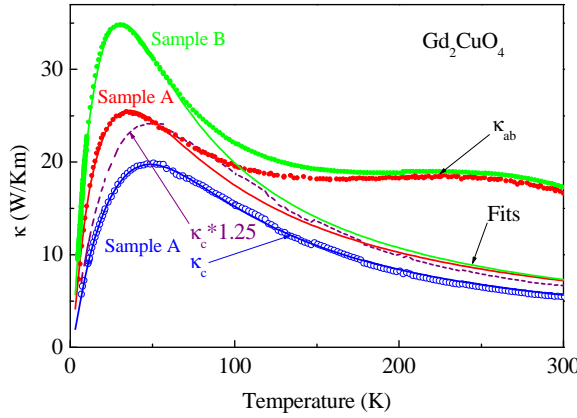


FIG. 1: (Color online) In-plane (κ_c) and out-of-plane (κ_{ab}) thermal conductivity of Gd_2CuO_4 . κ_{ab} was measured on two different crystals. Solid lines are fits by the Debye model and the dashed line is κ_c multiplied by a factor of 1.25 (see text).

temperature maxima of κ_{ab} strongly differ for the two crystals with $R = \text{Gd}$ indicating differences in the crystal quality, the magnitudes of their high-temperature maxima are almost identical. In Pr_2CuO_4 κ_{ab} also shows an additional high-temperature maximum, but its magnitude is less pronounced (see section V).

The double-peak structures of κ_{ab} cannot be modeled by the usual Debye model, but it is possible to describe the low-temperature maxima up to about 50 K. Comparing the corresponding fit parameters of κ_{ab} and κ_c (see Table I), the largest differences are found for the parameter D , which is significantly larger for the fits of κ_c

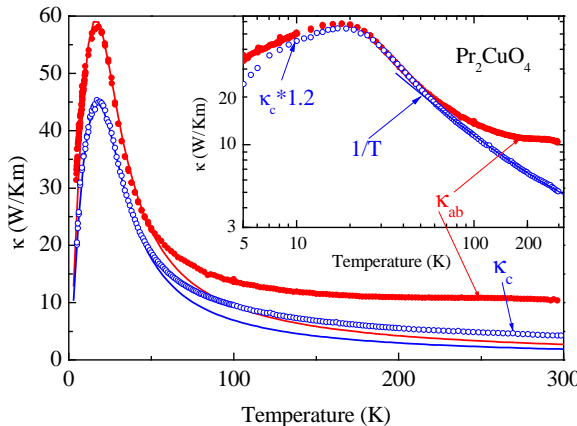


FIG. 2: (Color online) In-plane (κ_c) and out-of-plane (κ_{ab}) thermal conductivity of Pr_2CuO_4 . Lines are fits by the Debye model (see text). Inset: The same data on double-logarithmic scales with κ_c multiplied by a factor of 1.2. The temperature dependencies of κ_{ab} and κ_c around the low-temperature maxima are nearly the same. Above about 70 K κ_c follows a $1/T$ behavior (solid line), whereas an anomalous high-temperature upturn is present in κ_{ab} .

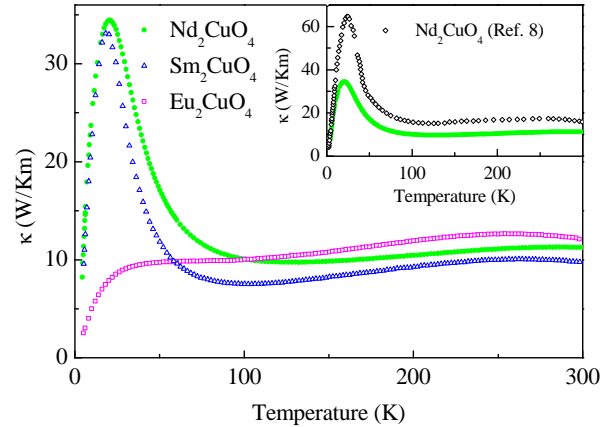


FIG. 3: (Color online) In-plane thermal conductivity of Nd_2CuO_4 , Sm_2CuO_4 , and Eu_2CuO_4 . For $R = \text{Eu}$ the low-temperature maximum is suppressed. The inset compares κ_{ab} (\bullet) of our Nd_2CuO_4 crystal with data (\circ) from Ref. 8.

than for those of κ_{ab} . This parameter gives the strength of phonon scattering by planar defects and it appears reasonable that due to the layered structure of $R_2\text{CuO}_4$ scattering by planar defects should be more effective for a heat current perpendicular to the planes than for j_H within the planes. Thus we interpret the different magnitudes of the low-temperature maxima of κ_c and κ_{ab} as a consequence of the layered structure. The high-temperature maxima of κ_{ab} around 250 K will be discussed in section V.

B. Nd_2CuO_4 , Sm_2CuO_4 , and Eu_2CuO_4

In Fig. 3 we show the in-plane thermal conductivities κ_{ab} of Nd_2CuO_4 , Sm_2CuO_4 , and Eu_2CuO_4 . The data for $R = \text{Nd}$ and Sm are very similar to each other and also to those of $R = \text{Pr}$ and Gd . In all crystals κ_{ab} exhibits a well defined low-temperature peak around 20 K and an additional broad maximum around 250 K. For $R = \text{Nd}$ similar results have been obtained by Jin *et al.*⁸, but κ_{ab} of our crystal is systematically lower in the entire temperature range (see Inset of Fig. 3). For Eu_2CuO_4 the low-temperature peak of κ_{ab} is almost completely suppressed. As described above, for $R = \text{Eu}$ the structural transition takes place at 170 K. The suppression of the low-temperature peak is most probably a consequence of this structural instability, which prevents a strong increase of the phonon mean free path at low temperatures. In contrast, however, the high-temperature maximum of κ_{ab} is hardly affected by this structural transition. The high-temperature maximum for Eu_2CuO_4 is even more pronounced than for the structurally stable crystals with $R = \text{Nd}$ and Sm .

V. DISCUSSION

Our data of κ_c of Pr_2CuO_4 and Gd_2CuO_4 together with κ_c of La_2CuO_4 (Refs. 11,12,13,14) clearly reveal that, on the one hand, the out-of-plane thermal conductivities of all these compounds of slightly different structures (tetragonal and orthorhombic T' , and orthorhombic T) do not exhibit any indications of an anomalous high-temperature contribution. On the other hand, all in-plane conductivities clearly show additional broad high-temperature maxima. The fact that these high-temperature maxima are present in crystals without ($R_2\text{CuO}_4$ with $R = \text{Pr}$, Nd , Sm , and $\text{Sr}_2\text{CuO}_2\text{Cl}_2$) or with (different) structural instabilities (T : $R = \text{La}$; T' : $R = \text{Eu}$ and Gd) unambiguously shows that the anomalous contribution to κ_{ab} does not depend on the existence of structural instabilities. This complements our previous suggestion based on a comparative study of κ of $\text{Sr}_2\text{CuO}_2\text{Cl}_2$ and La_2CuO_4 and, as we have discussed in detail in Ref. 17, the most natural explanation for the high-temperature maximum of κ_{ab} is an additional contribution to the heat transport caused by magnetic excitations.

The similar behavior of κ for all $R_2\text{CuO}_4$ confirms that such a magnetic contribution κ_{mag} to the in-plane heat transport is indeed an intrinsic property of the CuO_2 planes. It remains, however, to clarify what determines the magnitude of κ_{mag} . For a quantitative analysis we consider the in-plane thermal conductivity as the sum of a phononic and a magnetic contribution

$$\kappa_{ab} = \kappa_{ph} + \kappa_{mag}, \quad (1)$$

which are only weakly coupled to each other. In general, such an Ansatz can be used when the characteristic energy scales for the two contributions are well separated from each other. For example, this is usually the case for electronic and phononic heat transport since the Fermi temperature is much larger than the Debye temperature, i.e. $T_F \gg \Theta_D$. In the case of $R_2\text{CuO}_4$ it is a priori not clear whether the assumption of weakly coupled phononic and magnetic contributions is fulfilled, since the magnetic coupling J is only about four times as large as Θ_D (see Table I). However, the experimental observation that κ_{ab} shows two characteristic maxima, which are well separated from each other, encourages us to use Eq. (1).

In order to separate κ_{mag} from κ_{ab} we assume that in the region of the low-temperature peak κ_{mag} is negligibly small and fit the data for $T < 50\text{ K}$ (Gd_2CuO_4 ; $T < 85\text{ K}$) by the Debye model (see Eq. (1) of Ref. 17) and subtract the extrapolation of the fit from the measured data up to room temperature, i.e. $\kappa_{mag} = \kappa_{ab} - \kappa_{ph}^{fit}$.⁴⁰ This analysis is not possible for Eu_2CuO_4 , because the low-temperature maximum is not well-enough pronounced. However, even without a fit we expect rather similar values of κ_{mag} for $R = \text{Nd}$, Sm , and Eu , because the high-temperature data of κ_{ab} are very similar for these crystals (see Fig. 3). One can check the applicability of the Debye model to describe the phononic

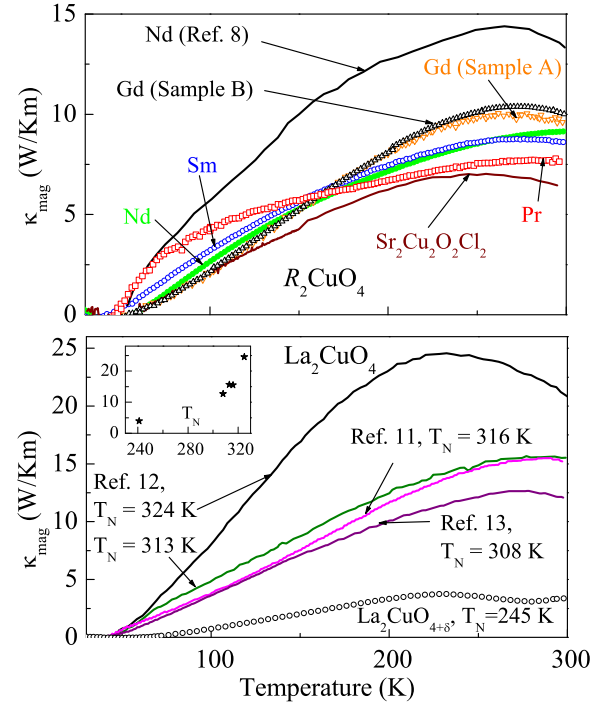


FIG. 4: (Color online) Magnetic contributions to the in-plane thermal conductivity, calculated via $\kappa_{mag} = \kappa_{ab} - \kappa_{ph}$, where κ_{ph} is determined by a Debye fit of the low-temperature maximum. Upper panel: Values calculated from our measurements of κ_{ab} of $R_2\text{CuO}_4$ and from the data from Ref. 8. Lower panel: The same analysis for various data of $\text{La}_2\text{CuO}_{4+\delta}$ taken from Refs. 11,12,13 and of our crystal with $T_N = 245\text{ K}$. Inset: The maximum of the calculated κ_{mag} vs. the Néel temperature for $\text{La}_2\text{CuO}_{4+\delta}$ (see text).

contribution by corresponding fits of κ_c , i.e. we restrict the temperature range of the fit to the low-temperature maxima and then compare the high-temperature extrapolations of the fits to the measured κ_c . As shown in Figs. 1 and 2 these fits yield a good description of κ_c for $R = \text{Gd}$ over the entire temperature range, whereas in the case of Pr the high-temperature values of κ_c are slightly underestimated by the fit. This probably arises from the sharper low-temperature peak for $R = \text{Pr}$. Since the low-temperature peaks of κ_{ab} for $R = \text{Pr}$, Nd , and Sm are also rather sharp, one may expect that the corresponding Debye fits will also underestimate the high-temperature values of the phononic contribution of κ_{ab} and consequently the magnetic contributions κ_{mag} may be overestimated to some extent.

In the upper panel of Fig. 4 we compare the resulting κ_{mag} of all our $R_2\text{CuO}_4$ crystals, our previous result of $\text{Sr}_2\text{CuO}_2\text{Cl}_2$ (Ref. 17), and κ_{mag} obtained from an analysis of κ_{ab} measured on Nd_2CuO_4 (Ref. 8). For comparison, we also show κ_{mag} obtained from the literature data of various La_2CuO_4 crystals.^{11,12,13} Obviously, the temperature dependence of κ_{mag} is very similar for all crys-

tals, but the magnitude of the broad maximum varies between about 7 and 10 W/Km for our $\text{Sr}_2\text{CuO}_2\text{Cl}_2$ and $R_2\text{CuO}_4$ crystals and from about 12 to 25 W/Km for the various crystals from literature with $R = \text{La}$ and Nd .^{8,11,12,13} Although these differences are not too large, we do not think that they simply arise from the experimental uncertainty in the quantitative determination of κ_{mag} .

Because the magnetic properties are rather similar for the different crystals, we expect that the different κ_{mag} mainly arise from differences in the scattering of the magnetic excitations. Possible scattering mechanisms are scattering between magnetic excitations and scattering by defects, phonons, and charge carriers. One may suspect that scattering between magnetic excitations, comparable e.g. to phonon-phonon Umklapp scattering, plays the most important role with respect to the temperature dependence of κ_{mag} . A deeper analysis of this scattering requires a detailed theoretical model for the dynamics of magnetic excitations, but even without such a model one may conclude that the similar magnetic properties naturally explain the similar temperature dependencies of κ_{mag} of the different compounds.

The influence of defects and charge carriers on the thermal conductivity has been investigated in Zn- and Sr-doped La_2CuO_4 .^{13,14} It has been found that Sr doping suppresses κ_{mag} much stronger than Zn doping and κ_{mag} vanishes almost completely above about 1% Sr. For both dopings the magnetic system is diluted, either by replacing magnetic Cu^{2+} by nonmagnetic Zn^{2+} ions or by the formation of Zhang-Rice singlets due to the introduced holes. However, the mobility of the holes strongly enhances the effect of charge-carrier doping, what is also reflected in a much stronger suppression of T_N by Sr doping as compared to Zn doping.⁴¹ As shown in the lower panel of Fig. 4, the magnitude of κ_{mag} for the various nominally undoped La_2CuO_4 crystals varies by about a factor of two. Since it is known that $\text{La}_2\text{CuO}_{4+\delta}$ is likely to have some excess oxygen, we plot the maximum of κ_{mag} as a function of T_N , which is very sensitive to small amounts of δ (Inset of Fig. 4). The observed correlation between the magnitude of κ_{mag} and T_N is a clear indication that the different magnitudes of κ_{mag} arise from small amounts of charge carriers in the different crystals.^{12,42}

One may suspect that the higher values of κ_{mag} of $R_2\text{CuO}_4$ with $R = \text{La}$ and Nd from Refs. 8,11,12,13 in comparison to our crystals could result from a weak charge carrier doping in our crystals. The rather low $T_N \simeq 250$ K of our Pr_2CuO_4 crystal compared to the T_N values up to $\simeq 280$ K reported in literature^{37,38,39} supports this view. However, this argumentation can neither explain the low κ_{mag} of our Gd_2CuO_4 with a large $T_N \simeq 292$ K nor does it hold for $\text{Sr}_2\text{CuO}_2\text{Cl}_2$, which is commonly believed to be very stable with respect to charge carrier doping. Unfortunately, not much is known about possible variations of the oxygen content in $R_2\text{CuO}_4$. Irrespective of the question of the exact oxy-

gen stoichiometry, our finding that κ_{mag} is very similar in crystals with and without structural instabilities leads to the conclusion that scattering by phonons seems to play a minor role for the magnetic heat transport in the CuO_2 planes. This is most clearly seen in Eu_2CuO_4 where the phononic low-temperature peak of Eu_2CuO_4 is strongly suppressed by a structural instability whereas its magnetic high-temperature maximum is hardly affected.

VI. CONCLUSIONS

In summary, we have studied the thermal conductivity of the rare earth cuprates $R_2\text{CuO}_4$ for both, a heat current perpendicular ($R = \text{Pr}$ and Gd) and parallel ($R = \text{Pr}$, Nd , Sm , Eu , and Gd) to the CuO_2 planes. The out-of-plane thermal conductivity shows the typical temperature dependence of a purely phononic thermal conductivity with a low-temperature maximum, whose magnitude depends on the crystal quality. In contrast, the in-plane conductivity for all crystal exhibits a pronounced double-peak structure consisting (i) of a low-temperature peak similar to that of the out-of-plane thermal conductivity and (ii) of an anomalous high-temperature contribution with a broad maximum around 250 K. Such an anisotropy between the in-plane and the out-of-plane thermal conductivity is also found in La_2CuO_4 .^{11,12,13,14} The fact that the double-peak is present in the structurally stable $R_2\text{CuO}_4$ with $R = \text{Pr}$, Nd , and Sm unambiguously rules out the possibility that the double-peak structure is caused by a structural instability, which is present for $R = \text{La}$, Eu , and Gd . The qualitative anisotropy between the in-plane and the out-of-plane thermal conductivity and the rather similar high-temperature behavior of the out-of-plane thermal conductivity for all the different crystals gives clear evidence that this additional high-temperature contribution arises from a sizeable heat transport by magnetic excitations within the CuO_2 planes. Our analysis yields a magnetic contribution to the in-plane thermal conductivity between about 7 to 25 W/Km depending on the R system. In weakly doped La_2CuO_4 this magnetic contribution is strongly suppressed showing that scattering of magnetic excitations by mobile charge carriers plays an important role. In contrast, the structural instability does hardly influence the magnetic thermal conductivity indicating that scattering of magnetic excitations by soft or anharmonic phonons plays a minor role. In order to clarify the role of scattering between magnetic excitations theoretical models describing the dynamics of magnetic excitations would be highly desirable.

Acknowledgments

We acknowledge useful discussions with M. Braden, M. Grüninger, and A. Sologubenko. This work was supported by the Deutsche Forschungsgemeinschaft through

SFB 608. The work in Minsk was supported in part by the Belarussian Foundation for Fundamental Research by

grant No. BRFFI F05-129.

¹ A.V. Sologubenko, K. Gianno, H.R. Ott, U. Ammerahl, and A. Revcolevschi. *Phys. Rev. Lett.* **84**, 2714 (2000).

² C. Hess, C. Baumann, U. Ammerahl, B. Büchner, F. Heidrich-Meisner, W. Brenig, and A. Revcolevschi. *Phys. Rev. B* **64**, 184305 (2001).

³ A.V. Sologubenko, K. Gianno, H.R. Ott, A. Vietkine, and A. Revcolevschi. *Phys. Rev. B* **64**, 054412 (2001).

⁴ Y. Ando, J. Takeya, D.L. Sisson, S.G. Doettinger, I. Tanaka, R.S. Feigelson, and A. Kapitulnik. *Phys. Rev. B* **58**, R2913 (1998).

⁵ M. Hofmann, T. Lorenz, A. Freimuth, G.S. Uhrig, H. Kageyama, Y. Ueda, G. Dhaleine, and A.M. Revcolevschi. *Physica B* **312**, 597 (2002).

⁶ A.V. Sologubenko, S.M. Kazakov, H.R. Ott, T. Asano, and Y. Ajiro. *Phys. Rev. B* **68**, 094432 (2003).

⁷ B.C. Sales, M.D. Lumsden, S.E. Nagler, D. Mandrus, and R. Jin. *Phys. Rev. Lett.* **88**, 095901 (2002).

⁸ R. Jin, Y. Onose, Y. Tokura, D. Mandrus, P. Dai, and B.C. Sales. *Phys. Rev. Lett.* **91**, 146601 (2003).

⁹ S.Y. Li, L. Taillefer, C.H. Wang, and X.H. Chen. *Phys. Rev. Lett.* **95**, 156603 (2005).

¹⁰ M.A. Kastner, R.J. Birgeneau, G. Shirane, and Y. Endoh. *Rev. Mod. Phys.* **70**, 897 (1998).

¹¹ Y. Nakamura, S. Uchida, T. Kimura, N. Motohira, K. Kishio, K. Kitazawa, T. Arima, and Y. Tokura. *Physica C* **185-189**, 1409 (1991).

¹² J.-Q. Yan, J.-S. Zhou, and J.B. Goodenough. *Phys. Rev. B* **68**, 104520 (2003).

¹³ X.F. Sun, J. Takeya, S. Komiya, and Y. Ando. *Phys. Rev. B* **67**, 104503 (2003).

¹⁴ C. Hess, B. Büchner, U. Ammerahl, L. Colonescu, F. Heidrich-Meisner, W. Brenig, and A. Revcolevschi. *Phys. Rev. Lett.* **90**, 197002 (2003).

¹⁵ M. Hofmann, T. Lorenz, G.S. Uhrig, H. Kierspel, O. Zabara, A. Freimuth, H. Kageyama, and Y. Ueda. *Phys. Rev. Lett.* **87**, 047202 (2001).

¹⁶ J.L. Cohn, C.K. Lowe-Ma, and T.A. Vanderah. *Phys. Rev. B* **52**, R13134 (1995).

¹⁷ M. Hofmann, T. Lorenz, K. Berggold, M. Grüninger, A. Freimuth, G.S. Uhrig, and E. Brück. *Phys. Rev. B* **67**, 184502 (2003).

¹⁸ D.C. Johnston. *Normal-state magnetic properties of single-layer cuprate high-temperature superconductors and related materials*. Elsevier Science B.V. (1997).

¹⁹ M. Braden, W. Schnelle, W. Schwarz, N. Pyka, G. Heger, Z. Fisk, K. Gamayunov, I. Tanaka, and H. Kojima. *Z. Physik B* **94**, 29 (1994).

²⁰ M. Braden, W. Paulus, A. Cousson, P. Vigoureux, G. Heger, A. Goukassov, P. Bourges, and D. Petitgrand. *Europhys. Lett.* **25**, 625 (1994).

²¹ P. Vigoureux, A. Gukasov, S.N. Barilo, and D. Zhigunov. *Physica B* **234**, 815 (1997).

²² A.V. Sologubenko, D.F. Brewer, G. Ekopiedidis, and A.L. Thomson. *Physica B* **263-264**, 788 (1999).

²³ A.V. Inyushkin, A.N. Taldenkov, L.N. Demyanets, T.G. Uvarova, and A.B. Bykov. *Physica B* **194-196**, 479 (1994).

²⁴ S.L. Cooper, G. A. Thomas, A. J. Millis, P. E. Sulewski, J. Orenstein, D. H. Rapkine, S-W. Cheong, and P.L. Trevor. *Phys. Rev. B* **42**, R10785 (1990).

²⁵ Here, only room temperature values are listed because temperature dependent values are not available for all samples. Note that these values are slightly larger than the low-temperature data used in Ref. 17, which were obtained by bi-magnon-plus-phonon absorption from infrared spectroscopy for La_2CuO_4 and $\text{Sr}_2\text{CuO}_2\text{Cl}_2$.

²⁶ C.Y. Chen, R.J. Birgeneau, M.A. Kastner, N.W. Preyer, and T. Thio. *Phys. Rev. B* **43**, 392 (1991).

²⁷ R. Sachidanandam, T. Yildirim, A.B. Harris, A. Aharoni, and O. Entin-Wohlman. *Phys. Rev. B* **56**, 260 (1997).

²⁸ D. Petitgrand, S.V. Maleyev, Ph. Bourges, and A.S. Ivanov. *Phys. Rev. B* **59**, 1079 (1999).

²⁹ A. Junod. *in Physical Properties of High Temperature Superconductors* volume 2. D. M. Ginsberg (Ed.), World Scientific Singapore (1989).

³⁰ T. Suzuki, T. Fukase, S. Wakimoto, and K. Yamada. *Physica B* **284-288**, 479 (2000).

³¹ M.F. Hundley, J.D. Thompson, S-W. Cheong, Z. Fisk, and S.B. Oseroff. *Physica C* **158**, 102 (1989).

³² D.V. Fil, I.G. Kolobov, V.D. Fil, S.N. Barilo, and D.I. Zhigunov. *Czech. J. Phys.* **46**, Supp. 4, 2155 (1996).

³³ S.N. Barilo, D.I. Zhigunov, and S.V. Shiryaev. *Physico-Chemical Fundamentals of Growth and Properties of $R_{2-x}Me_x\text{CuO}_4$ ($Me=\text{Sr, Ce}$)*. In: *High Temp. Supercond* volume 1. H.S. Freyhardt, R. Flukiger, M. Peuckert, Informationsgesellschaft Verlag (1993).

³⁴ J. Mira, J. Rivas, D. Fiorani, R. Caciuffo, D. Rinaldi, C. Vázquez-Vázquez, J. Mahía, M.A. López-Quintela, and S.B. Oseroff. *Phys. Rev. B* **52**, 16020 (1995).

³⁵ P.W. Klamut. *Phys. Rev. B* **50**, 13009 (1994).

³⁶ J.D. Yu, Y. Inaguma, M. Itoh, M. Oguni, and T. Kyomen. *Phys. Rev. B* **54**, 7455 (1996).

³⁷ I.W. Sumarlin, J.W. Lynn, T. Chattopadhyay, S.N. Barilo, D.I. Zhigunov, and J.L. Peng. *Phys. Rev. B* **51**, 5824 (1995).

³⁸ M. Matsuda, K. Yamada, K. Kakurai, H. Kadowaki, T.R. Thurston, Y. Endoh, Y. Hidaka, R.J. Birgeneau, M.A. Kastner, P.M. Gehring, A.H. Moudden, and G. Shirane. *Phys. Rev. B* **42**, 10098 (1990).

³⁹ D.E. Cox, A.I. Goldman, M.A. Subramanian, J. Gopalakrishnan, and A.W. Sleight. *Phys. Rev. B* **40**, 6998 (1989).

⁴⁰ We do not treat θ_D , v_s and L as free fit parameters, but use experimentally determined values. If no experimental values are available as e.g. for Gd_2CuO_4 we took values similar to those obtained in the other compounds (see Table I). The resulting fits hardly change when the upper boundary of the temperature range is varied by ± 10 K.

⁴¹ M. Hücker, V. Kataev, J. Pommer, J. Haraß, A. Hosni, C. Pfletsch, R. Gross, and B. Büchner. *Phys. Rev. B* **59**, R725 (1999).

⁴² For stronger oxygen doping a simple determination of δ from the measured T_N is not possible, because for $\delta \gtrsim 0.01$ a phase separation into oxygen-rich and oxygen-poor regions occurs, which is accompanied by various phase transitions leading to a complex phase diagram.³⁶ The kink in κ_{ab} at $T \approx 290$ K in our $\text{La}_2\text{CuO}_{4+\delta}$ crystal is also related to this phase separation.